CHEMISTRY

$^{15}N_4$-1,2,4,5-tetrazines as potential molecular tags: Integrating bioorthogonal chemistry with hyperpolarization and unearthing *para*-N_2

Junu Bae,[1]* Zijian Zhou,[1]* Thomas Theis,[1†] Warren S. Warren,[1,2,3] Qiu Wang[1†]

Hyperpolarized magnetic resonance (HP-MR) is a powerful, sensitive, and noninvasive approach to visualize molecular structure, function, and dynamics in vitro and in vivo. Current applications of HP-MR mostly rely on hyperpolarization of target compounds in dedicated hyperpolarizers because biomolecules can typically not be hyperpolarized directly in vivo. The injected hyperpolarized probes often undergo multiple metabolic pathways in living systems, and it remains challenging to localize and identify specific targets with high chemical selectivity. To address these current limitations in HP-MR, we report a novel hyperpolarization tagging strategy that integrates bioorthogonal chemistry and hyperpolarization to achieve the specific hyperpolarization of targets. This strategy is demonstrated by studies of hyperpolarized $^{15}N_4$-1,2,4,5-tetrazines, which undergo rapid and selective cycloaddition with cyclooctyne to provide hyperpolarized $^{15}N_2$-containing cycloaddition products and hyperpolarized $^{15}N_2$ gas. This work not only suggests great potential of $^{15}N_4$-1,2,4,5-tetrazines as molecular tags in HP-MR imaging (HP-MRI) but also supports the production of hyperpolarized *para*-$^{15}N_2$ gas, a biologically and medically innocuous gas with great potential for HP-MRI. This bioorthogonal reaction–based hyperpolarization tagging strategy enables a new class of in vitro and in vivo applications.

INTRODUCTION

Hyperpolarized magnetic resonance (HP-MR) has been developed to overcome the low sensitivity of conventional MR, a limitation that arises from poor nuclear magnetization at thermal equilibrium (*1*). For example, at 7 T and 310 K, equilibrium ^{1}H nuclear magnetization is just 0.0024% (*2*); other interesting nuclei, such as ^{13}C and ^{15}N, have even lower gyromagnetic ratios, and thus, their MR detection is even more challenging. Hyperpolarization techniques induce nonequilibrium magnetization of target nuclei and therefore raise detectable signals by multiple orders of magnitude (*3*, *4*). Particularly attractive is HP-MR imaging (HP-MRI) using heteronuclei (for example, ^{13}C or ^{15}N), which offers more comprehensive structural information than ^{1}H nuclear MR (NMR) and allows signal detection for extended periods of time due to their longer relaxation time compared to ^{1}H (*5*). Examples geared toward tracing metabolism and biological functions in living organisms include endogenous molecular species and derivatives, such as pyruvate (*6*), glucose (*7*), and amino acids (*6*, *8*, *9*). Other molecular probes include ^{15}N-pyridine derivatives (*10*) for measuring pH and ^{13}C-labeled drugs for tracking pharmacokinetics (*11*).

Despite these exciting advances, typical hyperpolarized probes, when subjected to in vivo applications, may readily undergo multiple metabolic pathways and cannot be directed to specific targets with high chemical selectivity. Furthermore, current HP-MRI mostly relies on ex vivo hyperpolarization of molecular targets. Exploiting HP-MRI for endogenous macromolecules in living systems remains an important yet unsolved challenge.

Here, we develop a novel hyperpolarization tagging strategy that uses hyperpolarizable reactive precursors that can undergo bioorthogonal cycloaddition reactions to achieve specific identification and localization of target molecules (Fig. 1A). Bioorthogonal chemistry is a powerful approach for the study of biomolecules in real time in living systems. It relies on rapid chemical ligation reactions between two bioorthogonal functional groups that are added to a biological sample. These two bioorthogonal partners react with each other in a chemoselective manner, which means that they are inert to any other chemical entity present. Meanwhile, the bioorthogonal chemistry should occur fast, in quantitative yield, and should be compatible with living systems (*12*, *13*). Thus, bioorthogonal reaction–based hyperpolarization tagging appears as an attractive strategy that can selectively highlight and localize the target-containing bioorthogonal partner. Ideally, this marriage of hyperpolarized MR with bioorthogonal chemistry would enable molecular tracking of any biomolecule with the high signal-to-noise ratio afforded by hyperpolarization, simply by tagging it with the hyperpolarized reaction partner. Therefore, the development of a hyperpolarized probe that could participate in rapid bioorthogonal ligation has immense potential as a generally applicable and chemically specific tag for HP-NMR and HP-MRI.

We demonstrate the bioorthogonal reaction–promoted hyperpolarization of selected targets using 1,2,4,5-tetrazines as hyperpolarizable precursors (Fig. 1B). The use of 1,2,4,5-tetrazines is particularly advantageous because of its dual role in both hyperpolarization and bioorthogonal reactions. First, we demonstrate that the hyperpolarization of ^{15}N-labeled tetrazines can be achieved by SABRE-SHEATH (Signal Amplification by Reversible Exchange in Shield Enables Alignment Transfer to Heteronuclei) (*14*–*16*). This hyperpolarization method takes advantage of recent developments using spin order transfer from *para*-hydrogen (*para*-H_2) (*17*–*21*) at very low fields (approximately 1% of the Earth's field), using a comparatively simple setup (*16*, *22*). Second, we expect that the hyperpolarized 1,2,4,5-tetrazines react selectively and rapidly with strained azadienophiles by inverse-demand Diels-Alder (IEDDA) reaction, one of the fastest bioorthogonal reactions reported (*13*, *23*–*28*). 1,2,4,5-Tetrazines are well studied, and various tetrazine-tagged biomolecules have been successfully used in vivo and in vitro (*24*–*27*). Here, we show that $^{15}N_4$-1,2,4,5-tetrazine contributes to both hyperpolarization and bioorthogonal ligation by generating the hyperpolarized cycloaddition target product. Furthermore, the $^{15}N_4$-1,2,4,5-tetrazine–based

[1]Department of Chemistry, Duke University, Durham, NC 27708, USA. [2]Department of Physics, Duke University, Durham, NC 27708, USA. [3]Departments of Radiology and Biomedical Engineering, Duke University, Durham, NC 27708, USA.
*These authors contributed equally to this work.
†Corresponding author. Email: qiu.wang@duke.edu (Q.W.); thomas.theis@duke.edu (T.T.)

IEDDA generates hyperpolarized $^{15}N_2$ gas, a typically ignored by-product of the tetrazine ligation. Here, our hyperpolarization approach also allows for selective access to *para*- and *ortho*-$^{15}N_2$, two fundamentally interesting spin isomers of $^{15}N_2$ (*29*). In particular, *para*-$^{15}N_2$ gas is a biologically and medically innocuous gas with mathematical properties similar to *para*-H_2 (*30*). Although *para*-$^{15}N_2$ has no net signal, even weak transient bindings to transition metal catalysts (including some biocatalysts) would be expected to unlock the spin order and create magnetization (*31*). However, hyperpolarized *para*-$^{15}N_2$ has not been reported to the best of our knowledge. In summary, our study entails the hyperpolarization of $^{15}N_4$-1,2,4,5-tetrazines using SABRE-SHEATH, followed by cycloaddition of the hyperpolarized tetrazine with an azadienophile, which enables the generation of hyperpolarized $^{15}N_2$-labeled products and hyperpolarized $^{15}N_2$ gas (Fig. 1B).

RESULTS AND DISCUSSION

For this proof-of-concept study, our investigation focused on ^{15}N-labeled 3-phenyl-1,2,4,5-tetrazine, namely, 3-phenyl-(6-*H*)-$^{15}N_4$-1,2,4,5-tetrazine **1a** and 3-phenyl-(6-*D*)-$^{15}N_4$-1,2,4,5-tetrazine **1b** (Fig. 2A), to evaluate their potential as a dual tag for hyperpolarization and bioorthogonal reaction. These tetrazines were synthesized from ortho-ester precursors with $^{15}N_2$-hydrazine hydrate, as fully described in the Supplementary Materials.

Hyperpolarization of $^{15}N_4$-1,2,4,5-tetrazines

Hyperpolarization of **1a** and **1b** was examined by standard SABRE-SHEATH procedure, as reported in our recent studies (*22*). Two different hyperpolarized states for $^{15}N_4$-1,2,4,5-tetrazine **1a** were observed, depending on the chosen magnetic field at which the *para*-H_2 gas is applied to the sample (Fig. 2B). At very low magnetic fields (~0.4 μT), the ^{15}N spin pairs of the tetrazine are hyperpolarized in the triplet states and display in-phase signal upon detection at 8.45 T (that is, magnetization is hyperpolarized). Conversely, at a relatively broad range of slightly elevated magnetic fields (~0.2 mT < B < ~50 mT), we observe antiphase signals after a 90° pulse. In this case, scalar order is hyperpolarized in the tetrazine spin pairs, associated with singlet states on ^{15}N spin pairs; upon transfer to high magnetic field for detection, this scalar order is transformed into antialigned magnetization (**I·S** is adiabatically converted to I_z-S_z; see the Supplementary Materials for details) (*32*). Such a field-dependent selection of hyperpolarized states corroborates our previous work on the hyperpolarization of $^{15}N_2$-diazirines and $^{13}C_2$-pyridyl acetylenes (*33*).

For tetrazine **1a**, the signal enhancement over 8.45-T thermal measurements is up to 3000-fold (0.9% polarization). At 0.3 mT, the magnetization has a relaxation constant T_1 of 1.4 ± 0.1 min, and at the same field, the relaxation constant of the scalar order of the ^{15}N spin pairs (T_s) is 2.7 ± 0.3 min, indicating that the scalar order is protected from relaxation and has a lifetime about two times longer than magnetization. We also measured the enhancement level and lifetimes of the tetrazine **1b**, expecting that the replacement of the tetrazine proton with deuterium could affect enhancement and lifetime (*34*). The hyperpolarized scalar order yielded 2900-fold enhancement, with T_s calculated to be 2.1 ± 0.7 min at 0.3 mT (that is, no significant change in lifetime within the error of the measurement). Note that it was not possible to create the hyperpolarized magnetization for deuterated compound **1b** (or to measure its T_1) because the quadrupolar deuterium quenches hyperpolarization at microtesla fields (*16*).

Bioorthogonal reactions of hyperpolarized $^{15}N_4$-1,2,4,5-tetrazines and cyclooctyne

With hyperpolarization of tetrazines **1a** and **1b** established successfully, we examined whether the hyperpolarization could be retained in reaction products of IEDDA reactions. We chose strained cyclooctyne bicyclo[6.1.0]non-4-yn-9-ylmethanol **2** (*35*, *36*) as the reaction partner of tetrazine in our studies and confirmed the sufficiently rapid rate of this cycloaddition reaction at room temperature (completed within seconds; see the Supplementary Materials for details). In particular, the formation of a single pyridazine product allows for a straightforward analysis, excluding potential complexity from multiple products, which arise when other known azadienophile partners, such as *trans*-cyclooctene, are used (*13*, *23*). We obtained the thermal ^{15}N reference spectra of both reactant tetrazine **1a** (before reaction) and product **3a** (after IEDDA reaction) from which we observe a clear distinction between the reactant and product by their ^{15}N chemical shifts (Fig. 3A).

To best monitor the hyperpolarized signals involved in the cycloaddition, we modified our conventional SABRE-SHEATH hyperpolarization setup and enabled direct injection of compound **2** into the solution of hyperpolarized tetrazine by adding a capillary tube into the pressurized NMR tube (see the Supplementary Materials for details). Note that all signals observed for **3** in the following experiments originate from tetrazine **1** and not from the SABRE-SHEATH of the

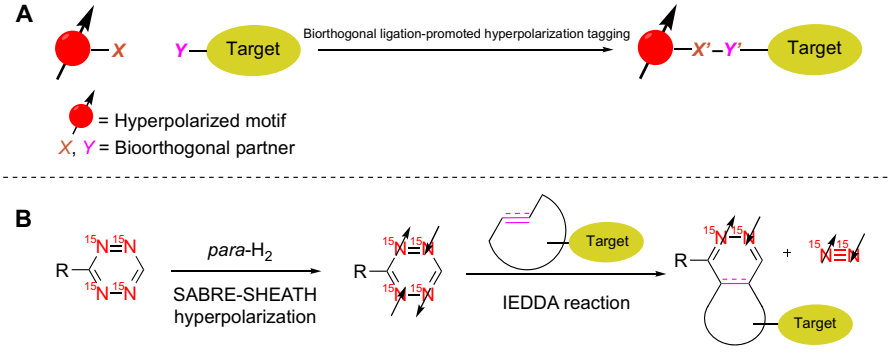

Fig. 1. A novel bioorthogonal reaction–promoted hyperpolarization tagging strategy. (**A**) Illustration of spin-hyperpolarized tagging via bioorthogonal chemistry. Bioorthogonal ligation between reactive partners *X* and *Y* incorporates the hyperpolarized chemical motif (red) within the target molecule (yellow). (**B**) $^{15}N_4$-1,2,4,5-tetrazine as a molecular tag and its dual roles in hyperpolarization and bioorthogonal ligation. First, the ^{15}N nuclei in $^{15}N_4$-1,2,4,5-tetrazine are hyperpolarized by SABRE-SHEATH, and then, the hyperpolarized tetrazine undergoes rapid IEDDA with a strained azadienophile, leading to the hyperpolarized $^{15}N_2$-cycloaddition product and hyperpolarized $^{15}N_2$ gas.

product. Control experiments attempting SABRE-SHEATH hyperpolarization of compound **3a** (the reaction product) provided no signal enhancements under the same conditions or even at higher temperatures with continuous bubbling of *para*-H_2.

We first examined the cycloaddition of **1a** after hyperpolarizing magnetization (that is, triplet states were hyperpolarized by bubbling at 0.4 μT before cycloaddition). After addition of a solution of **2** to a sample of hyperpolarized **1a** at 0.3 mT and subsequent transfer to high field, we observed sharp, in-phase peaks at 372 ppm that matched the position and pattern of the peaks observed in the thermal spectra of product **3a** (Fig. 3B). An additional signal was detected at 310 ppm, which corresponds to hyperpolarized $^{15}N_2$ gas (thermal spectrum of $^{15}N_2$ in CD_3OD is provided in the Supplementary Materials). These data reinforce that the IEDDA reaction of hyperpolarized $^{15}N_4$-tetrazine **1a** successfully generates hyperpolarized ^{15}N-containing products, including both $^{15}N_2$-pyridazine **3a** and $^{15}N_2$ gas. On the basis of the spectrum of hyperpolarized products, we calculated an enhancement of 540-fold over their thermal spectra. The magnetization lifetime T_1 for **3a** was determined to be 13 ± 4 s, substantially shorter than that of tetrazine **1a** (Fig. 3, C and D).

Next, we examined the reaction of **1a** after hyperpolarizing scalar order by bubbling at 0.3 mT (Fig. 3, E and F). After the solution of **2** was injected to the solution of hyperpolarized tetrazine at the same field (0.3 mT) and transferred to high field for detection, we observed antiphase peaks at 372 ppm, with 140-fold signal enhancements over thermal spectra. The T_s for **3a** was determined to be 13 ± 2 s, very similar in magnitude to T_1. This contrasts with the significant difference observed between T_1 and T_s for the tetrazine **1a**.

Furthermore, we examined the effects of deuteration in the cycloaddition reaction and products. As explained above, only scalar order

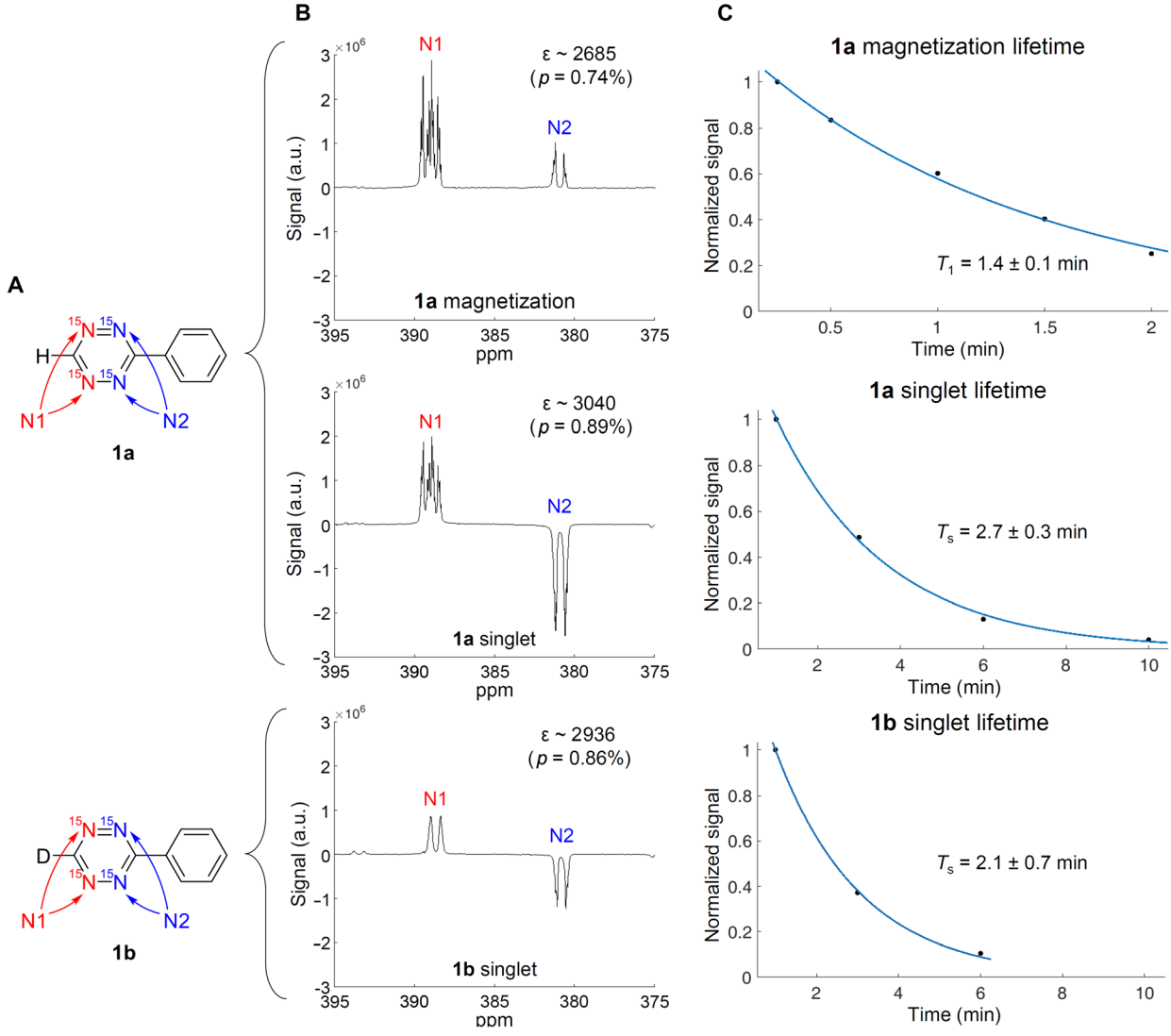

Fig. 2. Tetrazine hyperpolarization. (**A**) Structures of studied $^{15}N_4$-1,2,4,5-tetrazines **1a** and **1b**. (**B**) Single-shot hyperpolarized spectra of tetrazines **1a** and **1b** at magnetization or singlet modes, with peak identifications, observed enhancement (ε), and polarization level (*p*). Depending on the magnetic field at which hyperpolarization was induced, in-phase signal (magnetization) or antiphase signal (singlet) was observed. Enhancement values (ε) and polarization levels (*p*) were obtained by comparison of the hyperpolarized spectrum to a thermal reference spectrum of the respective $^{15}N_4$-1,2,4,5-tetrazine. a.u., arbitrary units; ppm, parts per million. (**C**) T_1 and T_s lifetime curves for **1a** and **1b**. Measurement at 0.3 mT. Sample as a solution of $^{15}N_4$-1,2,4,5-tetrazine (1.5 mM), pyridine (1.0 mM), and Ir(COD)(IMes)Cl [COD, 1,5-cyclooctadiene; IMes, 1,3-bis(2,4,6-trimethylphenyl) imidazol-2-ylidene; 0.15 mM] 0.15 mM] in methanol-d_4 (400 μl).

could be hyperpolarized on the deuterated tetrazine **1b**. Therefore, we were restricted to measurements of T_s in the deuterated product **3b**. Very similar to the observation in the reaction of tetrazine **1a**, antiphase peaks at 372 ppm were detected with a similar enhancement level of 180-fold. Encouragingly, a significantly longer lifetime T_s of 24 ± 6 s was obtained from the deuterated product (Fig. 3, G and H). This is expected because the deuterium couples less (6.5-fold less) into the $^{15}N_2$ spin system than ^1H (all relevant *J*-coupling parameters of **1a**, **1b**, **3a**, and **3b** are provided in the Supplementary Materials).

One key observation is that the $^{15}N_2$ gas signal at 310 ppm (Fig. 3, B and C) is absent with hyperpolarized scalar order (Fig. 3, E and G) after the cycloaddition reaction. The absence of nitrogen gas signals in these data provides indirect evidence for the generation of an intriguing new hyperpolarized species, *para*-nitrogen (*para*-$^{15}N_2$), that should have very

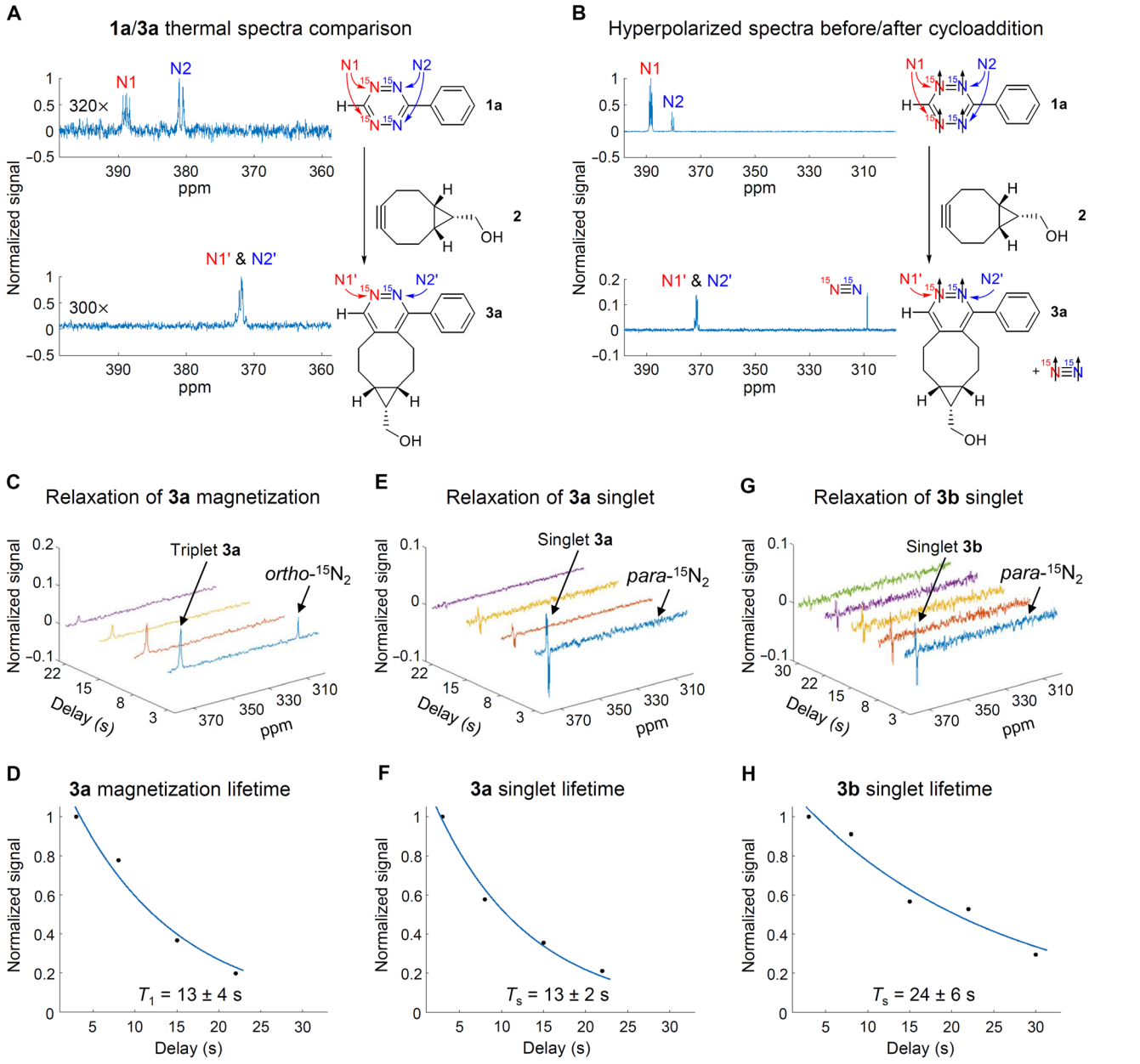

Fig. 3. IEDDA reaction and hyperpolarization transfer. (**A**) Thermal spectra of tetrazine **1a** compared to thermal spectra of cycloaddition product **3a**. Upon the cycloaddition reaction, a noticeable difference in chemical shift is observed on both nitrogen atoms (that is, N1 and N2 in **1a** versus N1′ and N2′ in **3a**). (**B**) Spectra of hyperpolarized **1a** and that obtained after the addition of **2**. Hyperpolarized **3a** and $^{15}N_2$ are observed. (**C**, **E**, and **G**) Representative T_1 or T_s decay measurements for product **3a** magnetization, **3a** singlet order, and **3b** singlet order, respectively. Note the presence of observable $^{15}N_2$ in the postaddition spectra when hyperpolarizing magnetization (C) but the absence of this peak in hyperpolarized singlet (E and G), which strongly suggests that singlet $^{15}N_2$ has been generated in these experiments. (**D**, **F**, and **H**) Lifetime measurement data, exponential fit of the data, and calculated T_1 or T_s values for product **3a** magnetization, **3a** singlet order, and **3b** singlet order, respectively. In the hyperpolarization-cycloaddition experiments, *para*-H_2 was bubbled into a solution of $^{15}N_4$-1,2,4,5-tetrazine **1a** or **1b** (1.5 mM), pyridine (1.0 mM), and Ir(COD)(IMes)Cl (0.15 mM) in methanol-d_4 (400 μl), and then, a solution of **2** (1.5 equiv.) in methanol-d_4 (200 μl) was added. The sample was held at 0.3 mT for a variable amount of time before transport to the magnet for detection.

similar spin properties to *para*-H_2, an extraordinary "quantum reagent" in a pure spin state. The H_2 molecule has an antisymmetric singlet state (*para*-H_2) and three symmetric "ortho" states. ^1H atoms are fermions; hence, they are antisymmetric with respect to exchange, so only *para*-H_2 can be in the (symmetric) ground rotational state $J = 0$ (*37*). The separation between $J = 0$ and $J = 1$ (in temperature units) is 174 K, so *para*-H_2 dominates at equilibrium at low temperatures. At room temperature in pure form, *para*-H_2 is extremely stable (100% *para*-H_2 drops to just 85% after 30 weeks) (*30*). With mathematical properties similar to *para*-H_2, *para*-$^{15}N_2$ can therefore be expected to be exceptionally long-lived as a promising MRI agent of clinical safety. However, *para*-$^{15}N_2$ cannot be prepared in the same way as *para*-H_2 because the rotational constant of N_2 is small and the nitrogen freezes before it achieves significant para excess under current conditions. Thus, the bioorthogonal reaction of hyperpolarized $^{15}N_4$-1,2,4,5-tetrazines represents a novel approach to permit characterization of this new quantum reagent.

To fully develop this bioorthogonal reaction–based hyperpolarization labeling strategy, we evaluated its feasibility under aqueous conditions toward in vivo biomedical applications. It should be noted that the SABRE-SHEATH hyperpolarization in water currently remains challenging, and its development is obstructed by a number of technical issues, including poor solubility of H_2 gas and iridium catalyst in water. Research to address these problems has been undertaken (*16*, *38*–*41*), including a strategy we recently reported to improve SABRE-SHEATH hyperpolarization in water using a water-soluble iridium catalyst and increased temperatures (60° to 70°C) (*42*). However, this strategy was not successful in our current studies because of the instability of the tetrazine at elevated temperatures. Encouragingly, with 3:1 CD_3OD/D_2O as a cosolvent system, we were able to achieve hyperpolarization of tetrazine **1a** with ~900-fold signal enhancement at 50°C and also detect the hyperpolarized signal from the cycloaddition product **3a** under these conditions (see the Supplementary Materials for details). These preliminary results pave the way toward application of this strategy under aqueous conditions, although more optimal SABRE-SHEATH hyperpolarization in water remains to be achieved.

CONCLUSION

We report a novel MR strategy by integrating bioorthogonal reactions and hyperpolarization. This strategy is demonstrated on the hyperpolarized $^{15}N_4$-1,2,4,5-tetrazines, which undergo rapid cycloaddition with cyclooctyne to provide hyperpolarized cycloaddition products and hyperpolarized $^{15}N_2$ gas. This work suggests great potential of $^{15}N_4$-1,2,4,5-tetrazines as powerful molecular tags in NMR and MRI, with dual roles in hyperpolarization and bioorthogonal ligation. Excitingly, the observations in the current study support the production of hyperpolarized $^{15}N_2$ gas in both its ortho and para spin isomers. Future studies will be directed toward systematic optimizations on the ^{15}N-tetrazine cycloaddition–based hyperpolarization tagging strategy and characterization of *para*-$^{15}N_2$ gas.

MATERIALS AND METHODS

Hyperpolarization setup

A high-pressure gas delivery system was specially built for the SABRE-SHEATH process. Normal H_2 gas was converted to *para*-H_2 (~90.2% enrichment) using a commercial *para*-H_2 generator. The *para*-H_2 gas was delivered to the sample solution through a capillary at a pressure of about 0.680 MPa (100 psi). The magnetically shielded environment was prepared using a three-layer μ-metal magnetic shield. A solenoid placed inside the shield controlled the magnetic field via manual adjustment of the voltage using a dc voltage output and a resistor. A separate capillary for the injection of a secondary solution was added adjacent to the *para*-H_2 delivery line, with a valve placed at the site of injection to seal the pressure when bubbling gas (see the Supplementary Materials for the diagram).

Sample preparation

For typical hyperpolarization experiments, a solution of ^{15}N-enriched tetrazine (**1a** or **1b**; 1.5 mM), pyridine (1.0 mM), and Ir(COD)(IMes)Cl (0.15 mM) in methanol-d_4 (400 μl) was prepared (*43*).

Tetrazine hyperpolarization procedure

The Ir catalyst was preactivated by bubbling *para*-H_2 through a solution of tetrazine, pyridine, and Ir catalyst (sample preparation described above) for 30 min. Following preactivation, the tetrazine was hyperpolarized, either by magnetization or by singlet order.

To hyperpolarize magnetization, the solution was placed inside the magnetic shield, with the magnetic field adjusted to 0.4 μT (using a solenoid of 430 mm with 205 turns and a voltage of 7.5 V across 11.4 kilohms). After 3 min of bubbling of *para*-H_2, the gas flow was stopped, and the sample was manually transferred from the low field to an 8.5-T spectrometer for signal readout as quickly as possible. This manual transfer took ~8 s, and a 90° pulse-acquire sequence was used for readout.

To hyperpolarize the singlet, the sample was placed at a magnetic field of 0.3 mT, and *para*-H_2 was bubbled through the solution for 3 min. As described in the above procedure, the sample was then manually transferred to an 8.5-T spectrometer as quickly as possible and detected using a 90° pulse-acquire sequence.

Tetrazine hyperpolarization and cycloaddition reaction procedure

For the hyperpolarization of the cycloaddition products **3a** and **3b**, a solution of tetrazine (**1a** or **1b**, respectively), pyridine, and Ir catalyst in methanol-d_4 was first hyperpolarized at 0.4 μT or 0.3 mT, depending on which spin order was studied (solution preparation and hyperpolarization procedure described above). After hyperpolarization, the *para*-H_2 gas flow was stopped, and the pressure was released through the exhaust outlet, after which the injection valve was quickly opened to inject a solution of cyclooctyne **2** (4.5 mM) in methanol-d_4 (200 μl) (1.5 equiv. of 2 with respect to tetrazine). Injection was completed in less than 1 s, and the sample was shaken for 3 s to reach complete reaction, visually evidenced by the color change from pink (that is, the color of the tetrazine) to transparent. The sample was then manually transferred to an 8.5-T spectrometer for product signal readout.

SUPPLEMENTARY MATERIALS

Supplementary material for this article is available at http://advances.sciencemag.org/cgi/content/full/4/3/eaar2978/DC1

Synthesis and cycloaddition reactions of 1,2,4,5-tetrazines

Hyperpolarization experiments

^1H, ^{13}C, and ^{15}N spectra

fig. S1. ^1H NMR comparison between tetrazine and cycloaddition product.

fig. S2. Experimental setup for hyperpolarization and hyperpolarized reaction experiments.

fig. S3. Hyperpolarized signal decay of magnetization and singlet at variable concentrations.

fig. S4. Hyperpolarization of magnetization and singlet as a function of magnetic field.

fig. S5. Comparison of the originally hyperpolarized singlet and diluted signal.

fig. S6. Small-tip-angle spectra of the hyperpolarized cycloaddition product **3a**.
fig. S7. SABRE-SHEATH experiment using methanol-d_4/D_2O mixture as solvent.
table S1. Magnetization and singlet enhancements and lifetimes at variable concentrations.
References (*44*, *45*)

REFERENCES AND NOTES

1. P. Nikolaou, B. M. Goodson, E. Y. Chekmenev, NMR hyperpolarization techniques for biomedicine. *Chemistry* **21**, 3156–3166 (2015).
2. N. K. Logothetis, What we can do and what we cannot do with fMRI. *Nature* **453**, 869–878 (2008).
3. J. H. Ardenkjaer-Larsen, B. Fridlund, A. Gram, G. Hansson, L. Hansson, M. H. Lerche, R. Servin, M. Thaning, K. Golman, Increase in signal-to-noise ratio of > 10,000 times in liquid-state NMR. *Proc. Natl. Acad. Sci. U.S.A.* **100**, 10158–10163 (2003).
4. R. V. Shchepin, A. M. Coffey, K. W. Waddell, E. Y. Chekmenev, Parahydrogen induced polarization of 1-^{13}C-phospholactate-d_2 for biomedical imaging with >30,000,000-fold NMR signal enhancement in water. *Anal. Chem.* **86**, 5601–5605 (2014).
5. G. Pileio, M. Carravetta, E. Hughes, M. H. Levitt, The long-lived nuclear singlet state of ^{15}N-nitrous oxide in solution. *J. Am. Chem. Soc.* **130**, 12582–12583 (2008).
6. M. J. Albers, R. Bok, A. P. Chen, C. H. Cunningham, M. L. Zierhut, V. Y. Zhang, S. J. Kohler, J. Tropp, R. E. Hurd, Y.-F. Yen, S. J. Nelson, D. B. Vigneron, J. Kurhanewicz, Hyperpolarized ^{13}C lactate, pyruvate, and alanine: Noninvasive biomarkers for prostate cancer detection and grading. *Cancer Res.* **68**, 8607–8615 (2008).
7. T. B. Rodrigues, E. M. Serrao, B. W. C. Kennedy, D.-E. Hu, M. I. Kettunen, K. M. Brindle, Magnetic resonance imaging of tumor glycolysis using hyperpolarized ^{13}C-labeled glucose. *Nat. Med.* **20**, 93–97 (2014).
8. C. Cabella, M. Karlsson, C. Canapè, G. Catanzaro, S. Colombo Serra, L. Miragoli, L. Poggi, F. Uggeri, L. Venturi, P. R. Jensen, M. H. Lerche, F. Tedoldi, In vivo and in vitro liver cancer metabolism observed with hyperpolarized [5-^{13}C]glutamine. *J. Magn. Reson.* **232**, 45–52 (2013).
9. P. R. Jensen, M. Karlsson, S. Meier, J. Ø. Duus, M. H. Lerche, Hyperpolarized amino acids for in vivo assays of transaminase activity. *Chemistry* **15**, 10010–10012 (2009).
10. W. Jiang, L. Lumata, W. Chen, S. Zhang, Z. Kovacs, A. D. Sherry, C. Khemtong, Hyperpolarized ^{15}N-pyridine derivatives as pH-sensitive MRI agents. *Sci. Rep.* **5**, 9104 (2015).
11. M. H. Lerche, S. Meier, P. R. Jensen, S.-O. Hustvedt, M. Karlsson, J. Ø. Duus, J. H. Ardenkjær-Larsen, Quantitative dynamic nuclear polarization-NMR on blood plasma for assays of drug metabolism. *NMR Biomed.* **24**, 96–103 (2011).
12. E. M. Sletten, C. R. Bertozzi, Bioorthogonal chemistry: Fishing for selectivity in a sea of functionality. *Angew. Chem. Int. Ed.* **48**, 6974–6998 (2009).
13. D. M. Patterson, L. A. Nazarova, J. A. Prescher, Finding the right (bioorthogonal) chemistry. *ACS Chem. Biol.* **9**, 592–605 (2014).
14. L. S. Bouchard, S. R. Burt, M. S. Anwar, K. V. Kovtunov, I. V. Koptyug, A. Pines, NMR imaging of catalytic hydrogenation in microreactors with the use of para-hydrogen. *Science* **319**, 442–445 (2008).
15. R. W. Adams, J. A. Aguilar, K. D. Atkinson, M. J. Cowley, P. I. P. Elliott, S. B. Duckett, G. G. R. Green, I. G. Khazal, J. López-Serrano, D. C. Williamson, Reversible interactions with para-hydrogen enhance NMR sensitivity by polarization transfer. *Science* **323**, 1708–1711 (2009).
16. D. A. Barskiy, R. V. Shchepin, C. P. N. Tanner, J. F. P. Colell, B. M. Goodson, T. Theis, W. S. Warren, E. Y. Chekmenev, The absence of quadrupolar nuclei facilitates efficient ^{13}C hyperpolarization via reversible exchange with parahydrogen. *ChemPhysChem* **18**, 1493–1498 (2017).
17. C. R. Bowers, D. P. Weitekamp, Transformation of symmetrization order to nuclear-spin magnetization by chemical-reaction and nuclear-magnetic-resonance. *Phys. Rev. Lett.* **57**, 2645–2648 (1986).
18. C. R. Bowers, D. P. Weitekamp, Parahydrogen and synthesis allow dramatically enhanced nuclear alignment. *J. Am. Chem. Soc.* **109**, 5541–5542 (1987).
19. T. C. Eisenschmid, R. U. Kirss, P. P. Deutsch, S. I. Hommeltoft, R. Eisenberg, J. Bargon, R. G. Lawler, A. L. Balch, Para hydrogen induced polarization in hydrogenation reactions. *J. Am. Chem. Soc.* **109**, 8089–8091 (1987).
20. I. V. Koptyug, K. V. Kovtunov, S. R. Burt, M. S. Anwar, C. Hilty, S.-I. Han, A. Pines, R. Z. Sagdeev, *para*-Hydrogen-induced polarization in heterogeneous hydrogenation reactions. *J. Am. Chem. Soc.* **129**, 5580–5586 (2007).
21. T. Theis, M. L. Truong, A. M. Coffey, R. V. Shchepin, K. W. Waddell, F. Shi, B. M. Goodson, W. S. Warren, E. Y. Chekmenev, Microtesla SABRE enables 10% nitrogen-15 nuclear spin polarization. *J. Am. Chem. Soc.* **137**, 1404–1407 (2015).
22. T. Theis, G. X. Ortiz Jr., A. W. J. Logan, K. E. Claytor, Y. Feng, W. P. Huhn, V. Blum, S. J. Malcolmson, E. Y. Chekmenev, Q. Wang, W. S. Warren, Direct and cost-efficient hyperpolarization of long-lived nuclear spin states on universal $^{15}N_2$-diazirine molecular tags. *Sci. Adv.* **2**, e1501438 (2016).
23. M. L. Blackman, M. Royzen, J. M. Fox, Tetrazine ligation: Fast bioconjugation based on inverse-electron-demand Diels–Alder reactivity. *J. Am. Chem. Soc.* **130**, 13518–13519 (2008).
24. N. K. Devaraj, R. Weissleder, S. A. Hilderbrand, Tetrazine-based cycloadditions: Application to pretargeted live cell imaging. *Bioconjug. Chem.* **19**, 2297–2299 (2008).
25. A. C. Knall, C. Slugovc, Inverse electron demand Diels–Alder (iEDDA)-initiated conjugation: A (high) potential click chemistry scheme. *Chem. Soc. Rev.* **42**, 5131–5142 (2013).
26. J. Šečkutė, N. K. Devaraj, Expanding room for tetrazine ligations in the in vivo chemistry toolbox. *Curr. Opin. Chem. Biol.* **17**, 761–767 (2013).
27. Y. Kurra, K. A. Odoi, Y.-J. Lee, Y. Yang, T. Lu, S. E. Wheeler, J. Torres-Kolbus, A. Deiters, W. R. Liu, Two rapid catalyst-free click reactions for in vivo protein labeling of genetically encoded strained alkene/alkyne functionalities. *Bioconjug. Chem.* **25**, 1730–1738 (2014).
28. Y.-F. Yang, Y. Liang, F. Liu, K. N. Houk, Diels–Alder reactivities of benzene, pyridine, and di-, tri-, and tetrazines: The roles of geometrical distortions and orbital interactions. *J. Am. Chem. Soc.* **138**, 1660–1667 (2016).
29. C. Bloomquist, S. Zhdanovich, A. A. Milner, V. Milner, Directional spinning of molecules with sequences of femtosecond pulses. *Phys. Rev. A* **86**, 063413 (2012).
30. S. Wagner, Conversion rate of *para*-hydrogen to *ortho*-hydrogen by oxygen: Implications for PHIP gas storage and utilization. *MAGMA* **27**, 195–199 (2014).
31. P. L. Holland, Metal–dioxygen and metal–dinitrogen complexes: Where are the electrons? *Dalton Trans.* **39**, 5415–5425 (2010).
32. M. G. Pravica, D. P. Weitekamp, Net NMR alignment by adiabatic transport of parahydrogen addition products to high magnetic field. *Chem. Phys. Lett.* **145**, 255–258 (1988).
33. Z. Zhou, J. Yu, J. F. P. Colell, R. Laasner, A. Logan, D. A. Barskiy, R. V. Shchepin, E. Y. Chekmenev, V. Blum, W. S. Warren, T. Theis, Long-lived $^{13}C_2$ nuclear spin states hyperpolarized by parahydrogen in reversible exchange at microtesla fields. *J. Phys. Chem. Lett.* **8**, 3008–3014 (2017).
34. K. Shen, A. W. J. Logan, J. F. P. Colell, J. Bae, G. X. Ortiz Jr., T. Theis, W. S. Warren, S. J. Malcolmson, Q. Wang, Diazirines as potential molecular imaging tags: Probing the requirements for efficient and long-lived SABRE-induced hyperpolarization. *Angew. Chem. Int. Ed.* **56**, 12112–12116 (2017).
35. J. Sauer, D. K. Heldmann, J. Hetzenegger, J. Krauthan, H. Sichert, J. Schuster, 1,2,4,5-Tetrazine: Synthesis and reactivity in [4+2]cycloadditions. *European J. Org. Chem.* **1998**, 2885–2896 (1998).
36. W. Chen, D. Wang, C. Dai, D. Hamelberg, B. Wang, Clicking 1,2,4,5-tetrazine and cyclooctynes with tunable reaction rates. *Chem. Commun.* **48**, 1736–1738 (2012).
37. R. A. Green, R. W. Adams, S. B. Duckett, R. E. Mewis, D. C. Williamson, G. G. R. Green, The theory and practice of hyperpolarization in magnetic resonance using *para*hydrogen. *Prog. Nucl. Magn. Reson. Spectrosc.* **67**, 1–48 (2012).
38. M. Fekete, O. Bayfield, S. B. Duckett, S. Hart, R. E. Mewis, N. Pridmore, P. J. Rayner, A. Whitwood, Iridium(III) hydrido N-heterocyclic carbene–phosphine complexes as catalysts in magnetization transfer reactions. *Inorg. Chem.* **52**, 13453–13461 (2013).
39. M. L. Truong, F. Shi, P. He, B. Yuan, K. N. Plunkett, A. M. Coffey, R. V. Shchepin, D. A. Barskiy, K. V. Kovtunov, I. V. Koptyug, K. W. Waddell, B. M. Goodson, E. Y. Chekmenev, Irreversible catalyst activation enables hyperpolarization and water solubility for NMR signal amplification by reversible exchange. *J. Phys. Chem. B* **118**, 13882–13889 (2014).
40. H. Zeng, J. Xu, M. T. McMahon, J. A. B. Lohman, P. C. M. van Zijl, Achieving 1% NMR polarization in water in less than 1 min using SABRE. *J. Magn. Reson.* **246**, 119–121 (2014).
41. P. Rovedo, S. Knecht, T. Bäumlisberger, A. L. Cremer, S. B. Duckett, R. E. Mewis, G. G. R. Green, M. Burns, P. J. Rayner, D. Leibfritz, J. G. Korvink, J. Hennig, G. Pütz, D. von Elverfeldt, J.-B. Hövener, Molecular MRI in the Earth's magnetic field using continuous hyperpolarization of a biomolecule in water. *J. Phys. Chem. B* **120**, 5670–5677 (2016).
42. J. F. P. Colell, M. Emondts, A. W. J. Logan, K. Shen, J. Bae, R. V. Shchepin, G. X. Ortiz Jr., P. Spannring, Q. Wang, S. J. Malcolmson, E. Y. Chekmenev, M. C. Feiters, F. P. J. T. Rutjes, B. Blümich, T. Theis, W. S. Warren, Direct hyperpolarization of nitrogen-15 in aqueous media with parahydrogen in reversible exchange. *J. Am. Chem. Soc.* **139**, 7761–7767 (2017).
43. M. J. Cowley, R. W. Adams, K. D. Atkinson, M. C. R. Cockett, S. B. Duckett, G. G. R. Green, J. A. B. Lohman, R. Kerssebaum, D. Kilgour, R. E. Mewis, Iridium N-heterocyclic carbene complexes as efficient catalysts for magnetization transfer from *para*-hydrogen. *J. Am. Chem. Soc.* **133**, 6134–6137 (2011).
44. J. L. Markley, A. Bax, Y. Arata, C. W. Hilbers, R. Kaptein, B. Sykes, P. E. Wright, K. Wüthrich, Recommendations for the presentation of NMR structures of proteins and nucleic acids (IUPAC Recommendations 1998). *Pure Appl. Chem.* **70**, 117–142 (1998).
45. W. Kong, Q. Wang, J. Zhu, Palladium-catalyzed enantioselective domino heck/intermolecular C–H bond functionalization: Development and application to the synthesis of (+)-esermethole. *J. Am. Chem. Soc.* **137**, 16028–16031 (2015).

Acknowledgments
Funding: This work was supported by the NSF (grants CHE-1363008 to W.S.W. and CHE-1665090 to W.S.W. and T.T.), the Alfred P. Sloan Foundation (to Q.W.), and the Camille and Henry Dreyfus Foundation (to Q.W.), and Duke University. J.B. acknowledges the Graduate Assistance in Areas of National Need fellowship support. **Author contributions:** J.B. performed the chemistry experiments. J.B. and Z.Z. performed the hyperpolarization experiments. Q.W. conceived the project. T.T., W.S.W., and Q.W. supervised the project. All authors contributed to the experimental designs. J.B. and Q.W. wrote the manuscript with feedbacks from Z.Z., T.T., and W.S.W. **Competing interests:** The authors declare that they have no competing interests. **Data and materials availability:** All data needed to evaluate the conclusions in the paper are present in the paper and/or the Supplementary Materials.

Questions concerning spin dynamics and hyperpolarization physics should be directed to T.T. Correspondence and requests for materials should be addressed to Q.W.

Submitted 23 October 2017
Accepted 1 February 2018
Published 9 March 2018
10.1126/sciadv.aar2978

Citation: J. Bae, Z. Zhou, T. Theis, W. S. Warren, Q. Wang, $^{15}N_4$-1,2,4,5-tetrazines as potential molecular tags: Integrating bioorthogonal chemistry with hyperpolarization and unearthing *para*-N_2. *Sci. Adv.* **4**, eaar2978 (2018).